

Spherical ‘Top-Hat’ Collapse in general Chaplygin gas dominated universes

R. A. A. Fernandes,^{1,2,*} J. P. M. de Carvalho,^{3,1} A. Yu. Kamenshchik,^{4,5} U. Moschella,^{2,6} and A. da Silva¹

¹*Centro de Astrofísica, Universidade do Porto,
Rua das Estrelas, 4150-762 Porto, Portugal*

²*Dipartimento di Scienze Matematiche,
Fisiche e Chimiche, Università dell’Insubria,
Via Valleggio 11, 22100 Como, Italy*

³*Departamento de Matemática da Faculdade Ciências da Universidade do Porto,
Rua do Campo Alegre, 4169-007 Porto, Portugal*

⁴*Physics Department and INFN, University of Bologna,
via Irnerio 46, 40126 Bologna, Italy*

⁵*L.D. Landau Institute for Theoretical Physics of the Russian Academy of Sciences,
Kosygina str. 2, 119334 Moscow, Russia*

⁶*INFN, Sez di Milano*

(Dated: July 10, 2018)

Abstract

We expand previous works on the spherical ‘top-hat’ collapse (SC-TH) framework in generalized Chaplygin gas (gCg) dominated universes. Here we allow the collapse in all energetic components within the system. We analyze the non-linear stages of collapse for various choices of parameter α of the gCg model introducing an exact formulation for the so-called effective sound speed, c_{eff}^2 . We show that, within the SC-TH framework, the growth of the structure becomes faster with increasing values of α .

PACS numbers: 98.80.-k., 95.36.+x, 95.35.+d

* Electronic address: Rui.Fernandes@astro.up.pt

I. INTRODUCTION

More than a decade has passed since Type Ia Supernovae observations provided a first indication of the present accelerated expansion of the Universe [1, 2]. The culprit, Dark Energy (DE) - in the form of a cosmological constant - soon became the simplest way to describe this dynamical behavior. Since then, the amount of observational evidence supporting DE has grown in a way that it has become a major player in the concordance model of cosmology (for a review on DE see e.g. [3, 4]). Although DE accounts for $\sim 70\%$ of the present energy density of the Universe, its physical nature remains undisclosed. Another key player of the concordance model, whose nature is also unknown to particle physics, is dark matter (DM). Together with DE, they account for most (95%) of the present matter-energy density (the so called *dark sector*) of the Universe. While DE may be modeled as a fluid with negative pressure acting against gravitational collapse, DM (in its cold version) is a dust like fluid with no pressure, therefore enhancing the collapse of matter perturbations (for a review on DM see e.g. [5, 6]).

Although the cosmological constant is the simplest DE model that fits present astronomical data, understanding its nature poses most pressing challenges to particle physics and cosmology. Alternative DE models have been proposed to alleviate some of the problems of the cosmological constant concordance model. This include dynamical DE, minimally coupled or with interactions (see e.g. [7, 8]), and Unified Dark Models (UDM) (see e.g. [9, 10]). In the later case, DE and DM are described by the same physical entity. A particular UDM, first introduced in [11] and subsequently developed by [12–14], is the so-called *generalized Chaplygin gas* (gCg), which is based on the following exotic equation of state (EoS):

$$p = -\frac{C}{\rho^\alpha}, \quad (1)$$

where p is the pressure, ρ is the density, and C and α are constants (in general, both assumed to be positive). The $\alpha = 1$ case, corresponds to the standard Chaplygin gas, named after the Russian physicist Sergey A. Chaplygin who studied it in a hydrodynamical context [15].

Using Eq. (1) together with the relativistic energy-momentum conservation equation, one can show that gCg's background density evolution is (see e.g. [16]):

$$\rho = \rho_0 \left(\bar{C} + (1 - \bar{C})a^{-3(\alpha+1)} \right)^{\frac{1}{1+\alpha}}. \quad (2)$$

where $\bar{C} = C/\rho_0^{1+\alpha}$, ρ_0 is the density at the present epoch and a is the cosmic scale factor,

which is related to the cosmological redshift by $1 + z = 1/a$ (assuming the scale factor normalized for the present epoch, i.e. $a_0 = 1$).

It can be easily shown that the EoS parameter, $w = p/\rho$, is given by:

$$w = -\bar{C} \left(\bar{C} + (1 - \bar{C})a^{-3(\alpha+1)} \right)^{-1}. \quad (3)$$

Equation (3) shows that at early times (small a , high densities), w tends to zero, i.e. the gCg behaves as DM, whereas at later times w tends to -1 , i.e. the gCg behavior approaches the one expected for DE. It is worth noting that previous works on the global cosmological dynamics of gCg's dominated universes have shown consistency with SNIa, CMB and GRB observations (see e.g. [17–20]).

Past research on linear perturbation theory has shown that although not all values of α favor structure formation, there is still some degree of agreement between gCg UDM and large-scale structure observations (see e.g. [21–24]). However the validity of comparing linear theory results with observations has been questioned recently for the gCg UDM. In particular it has been noted in [23] that in gCg UDM non-linear effects generate a backreaction in the background dynamics that cannot be ignored, putting in this way serious constraints on the validity of linear theory as soon as the first scales become non-linear. It is fair to say that non-linear studies are required to state whether or not the gCg models can become a serious alternative to Λ CDM.

In [25], the authors have studied the non-linear evolution of dark matter and dark energy in the Chaplygin gas cosmology, using generalizations of the spherical model that incorporated effects of the acoustic horizon. An interesting phenomenon was found there: a fraction of the Chaplygin gas condensated and never reached a stage where its properties changed from dark-matter-like to dark-energy-like.

A fully non-linear analysis is a cumbersome task usually handled by hydrodynamical/N-body numerical codes (see e.g. [26–29]). However, to best of our knowledge, the gCg case has not yet been addressed, mainly due to its complex dynamical behavior.

In this paper we focus on the collapse of a spherically symmetric perturbation, with a classical top-hat profile, leaving the use of N-body techniques to study the non-linear evolution of gCg perturbations to further investigations.

We consider a Friedmann-Lemaître-Robertson-Walker (FLRW) universe with two energetic components: gCg and *baryons*; since our study is restricted to the post-recombination

epoch we neglect radiation. Our treatment allows the collapse of both *baryons* and gCg, at variance with previous works, see e.g. [25, 30, 31]. We further assume a time-dependent parameter $w \equiv w(t)$ for both the collapsing region and the background, and re-examine the definition of the *effective sound speed* of the perturbed region c_{eff}^2 . We derive a more accurate expression for c_{eff}^2 rather than using a approximation as in [32].

The paper is organized as follows: Section II describes the fundamental equations for the SC-TH framework and revises the notion of *effective sound speed*. Section III contains our numerical implementation and a discussion of the results. The paper ends with Section IV where we draw our conclusions. An appendix is added for completeness where we derive the main equations of the SC-TH model.

II. SPHERICAL ‘TOP HAT’ COLLAPSE OF CHAPLYGIN GAS

A. The basic equations

The spherical collapse provides a way to glimpse into the non-linear regime of perturbation theory, before using more complex methods like N-body simulations. Basically, the SC describes the evolution of a spherically symmetric perturbation embedded in a homogeneous background, which can be static, expanding or collapsing. One assumes a spherical ‘top hat’ profile for the perturbed region, i.e. a spherically symmetric perturbation in some region of space with constant density. The assumption of a ‘top hat’ profile further simplifies the SC model as the uniformity of the perturbation is maintained throughout the collapse, making its evolution only time dependent. As a consequence, we don’t need to worry about gradients inside the perturbed region. In essence, the spherical ‘top-hat’ collapse model (SC-TH) describes the evolution of a homogeneous mini-universe inside a larger homogeneous universe.

The basic equations used in the SC-TH model are the same that govern the cosmological background evolution (see e.g. [33–36]): the continuity equation

$$\dot{\rho} = -3H(\rho + p), \quad (4)$$

where $H = \dot{a}/a$ is the Hubble factor, and the Raychaudhuri equation

$$\frac{\ddot{a}}{a} = -\frac{4\pi G}{3} \sum_i (\rho_i + 3p_i). \quad (5)$$

where G is the gravitational constant and the $\sum_i(\rho_i + 3p_i)$ factor represents the total contribution, of density and pressure, from each individual component. Please note that in this work we normalize the speed of light to unity, i.e. $c = 1$. For the perturbed region, equations (4) and (5) are dependent on local quantities and can be written as

$$\dot{\rho}_c = -3h(\rho_c + p_c) \quad (6)$$

$$\frac{\ddot{r}}{r} = -\frac{4\pi G}{3} \sum_i(\rho_{c_i} + 3p_{c_i}). \quad (7)$$

where $h = \dot{r}/r$ and r are respectively the local expansion rate and the local scale factor; the perturbed quantities ρ_c and p_c are related to their background counterparts by:

$$\rho_c = \rho + \delta\rho \quad (8)$$

$$p_c = p + \delta p. \quad (9)$$

A simple relation between h and H can be derived under the SC–TH framework [36],

$$h = H + \frac{\theta}{3a} \quad (10)$$

where $\theta \equiv \vec{\nabla} \cdot \vec{v}$ and \vec{v} is the peculiar velocity field.

The equations governing the dynamical behavior of SC–TH are the following [36] (see the appendix):

$$\begin{aligned} \dot{\delta}_j &= -3H(c_{eff_j}^2 - w_j)\delta_j \\ &\quad - [1 + w_j + (1 + c_{eff_j}^2)\delta_j] \frac{\theta}{a}, \end{aligned} \quad (11)$$

$$\begin{aligned} \dot{\theta} &= -H\theta - \frac{\theta^2}{3a} \\ &\quad - 4\pi G a \sum_j \rho_j \delta_j (1 + 3c_{eff_j}^2), \end{aligned} \quad (12)$$

where $\delta_j = (\delta\rho/\rho)_j$ and $c_{eff_j}^2 = (\delta p/\delta\rho)_j$ are, respectively, the density contrast and the square of the effective sound speed in component j [37].

It must be noted that there are as many equations in (11) as the number of cosmological fluid components in the system, while Eq. (12) stands alone. This is true only because we are using a ‘top-hat’ profile, resulting in $\vec{\nabla} p = 0$; in a more general situation each cosmological component would satisfy a corresponding Euler’s equation. It is also convenient to use the scale factor a instead of the cosmic time t and the cosmological density parameters

Model	α	\bar{C}	z_{ta}	$\delta_b(z_{ta})/\delta_{gCg}(z_{ta})$
a	0	0.75	0.138	3.02
b	10^{-3}	0.75	0.140	3.00
c	10^{-2}	0.75	0.168	2.83
d	10^{-1}	0.75	0.371	1.96
e	0.5	0.75	0.685	1.20
f	1	0.75	0.774	1.05

TABLE I. Models used for the evaluation of the SC-TH model in gCg-dominated universes.

$\Omega_j = \frac{8\pi G}{3H^2}\rho_j$. After taking this into account we are left with the following set of equations:

$$\delta'_j = -\frac{3}{a}(c_{effj}^2 - w_j)\delta_j - [1 + w_j + (1 + c_{effj}^2)\delta_j]\frac{\theta}{a^2H}, \quad (13)$$

$$\theta' = -\frac{\theta}{a} - \frac{\theta^2}{3a^2H} - \frac{3H}{2} \sum_j \Omega_j \delta_j (1 + 3c_{effj}^2), \quad (14)$$

where the prime denotes the derivative with respect to a .

Another useful quantity is the redshift of turnaround z_{ta} which marks the instant when the perturbed region detaches itself from the background expansion and starts its collapsing stage (i.e. decreasing its physical radius). One can define z_{ta} as the redshift at which $h = 0$, i.e. $z_{ta} = z(h = 0)$.

B. On the effective sound speed

We now turn our attention to a decisive player in the dynamics of equations (13)–(14), the ratio $\delta p/\delta\rho = c_{eff}^2$. We argue that a correct computation of c_{eff}^2 is crucial to achieve coherent results and interpretations. Under some circumstances c_{eff}^2 can be numerically approximated by the square of the adiabatic sound speed, i.e. c_s^2 , but they are in fact two different quantities with clear different meanings. While c_s^2 is inherent to the fluid thermodynamics, the factor c_{eff}^2 only exists if a perturbation is present. Moreover, within a perturbed system, it is the value of the ratio $\delta p/\delta\rho = c_{eff}^2$ (and not $c_s^2 = \partial p/\partial\rho$), that

critically determines the dynamical behavior of the perturbed region.

The basic equation for the study of the SC–TH in a gCg-dominated universe relates the state parameter of the background w and the parameter relative to the collapsing region w_c as follows:

$$w_c = \frac{p + \delta p}{\rho + \delta \rho} = \frac{w}{1 + \delta} + c_{eff}^2 \frac{\delta}{1 + \delta}. \quad (15)$$

In [32] w_c is computed by approximating c_{eff}^2 by the adiabatic sound speed of the background (i.e. $c_s^2 = \partial p / \partial \rho = -\alpha w$), by trading a parameter of the perturbed region for a background one; this is a good approximation only if $\delta \ll 1$. However, clearly this is not the case at later stages of the collapse; in particular positive values for w_c result out of this approximation, in disagreement with the equation of state of the Chaplygin fluid (see, for instance, Fig. 1 in [32]).

Here we remove the approximation used in [32], and take a step forward in understanding of the SC in gCg-dominated universes. This amounts to writing c_{eff}^2 by using the EoS of the gCg (1), and the relation between the densities in the background and in the collapsed region as follows:

$$c_{eff}^2 = \frac{\delta p}{\delta \rho} = \frac{p_c - p}{\rho_c - \rho}; \quad (16)$$

by using $\rho_c = \rho(1 + \delta)$ and Eq. (1), one obtains

$$c_{eff}^2 = -\frac{C}{\rho^{1+\alpha}} \frac{(1 + \delta)^{-\alpha} - 1}{\delta} = w \frac{(1 + \delta)^{-\alpha} - 1}{\delta} \quad (17)$$

This relation shows an effective sound speed dependent on both the background and the collapsed region via w and δ respectively. It also shows that larger values of δ will result on smaller values of c_{eff}^2 , which is exactly the behavior one should expect in a gCg clump ($\delta \gg 1, w \sim 0, c_s^2 \sim 0$). Moreover, expanding the term $(1 + \delta)^{-\alpha}$ in a Taylor series, for small values of δ one can write

$$c_{eff}^2 = w \frac{1 - \alpha\delta + \mathcal{O}(2) - 1}{\delta} \simeq -\alpha w, \quad (18)$$

thus showing that as $\delta \rightarrow 0$ the value of $c_{eff}^2 \rightarrow c_s^2$, as expected. It is always possible to derive an expression for c_{eff}^2 , analogous to Eq. (17), for any DE model possessing an EoS of the type $p = p(\rho)$.

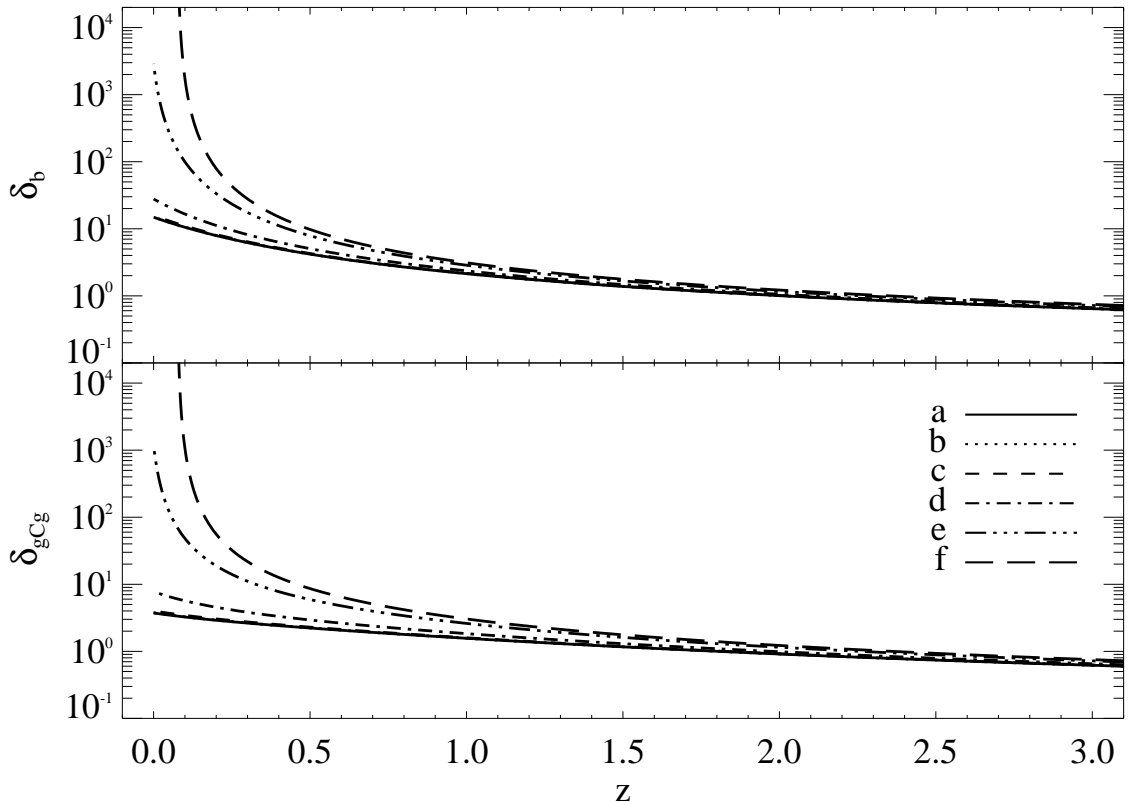


FIG. 1. Growth of perturbations for the SC – TH in gCg-dominated universes. *Top*: δ_b vs z . *Bottom*: δ_{gCg} vs z

Using the SC–TH framework and Eq. (1) it is also possible to compute directly w_c . Since gCg’s state parameter w , is given by

$$w = p/\rho = -\frac{C}{\rho^{1+\alpha}} \quad (19)$$

and that $\rho_c = \rho(1 + \delta)$, then w_c simply becomes

$$w_c = -\frac{C}{(\rho(1 + \delta))^{1+\alpha}} = \frac{w}{(1 + \delta)^{1+\alpha}} \quad (20)$$

Eq. (20) clearly shows that for a positive perturbation, i.e. $\delta > 0$, w_c goes to zero when δ increases. The decrease rate of w_c is dependent on the value of α , and higher values of α imply faster variations relative to the background value.

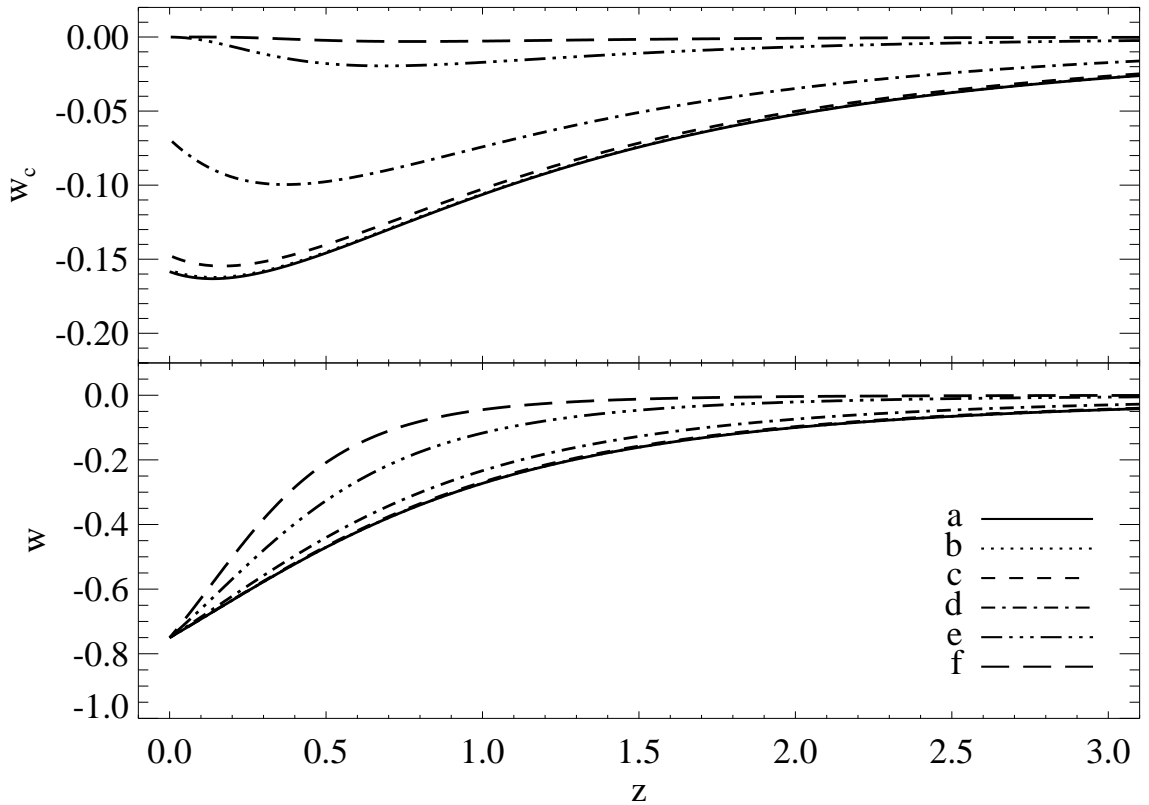


FIG. 2. gCg's w_c and w evolution with redshift for all the models presented in Table I. Higher values of α result in values of w_c closer to zero throughout the collapse and in a later transition from DM to DE dominated stages of the gCg universes.

III. THE NUMERICAL APPROACH

A. The method

Even though the gCg model has two free parameters, C and α , we expect that α has the largest ‘effective’ influence on the growth of perturbations within the SC–TH framework. Not only it is strongly connected to the effective sound speed of perturbations, but it also dictates for how long the DM stage of the gCg component lasts.

To investigate the effect of α on the growth of perturbations within the SC–TH framework, we integrate a system of Ordinary Differential Equations (ODE), for different values of α while keeping fixed the value of $\bar{C} = 0.75$. The chosen values of α for the numerical integration are shown in Table I (recall that model ‘a’ is equivalent to Λ CDM). The ODE

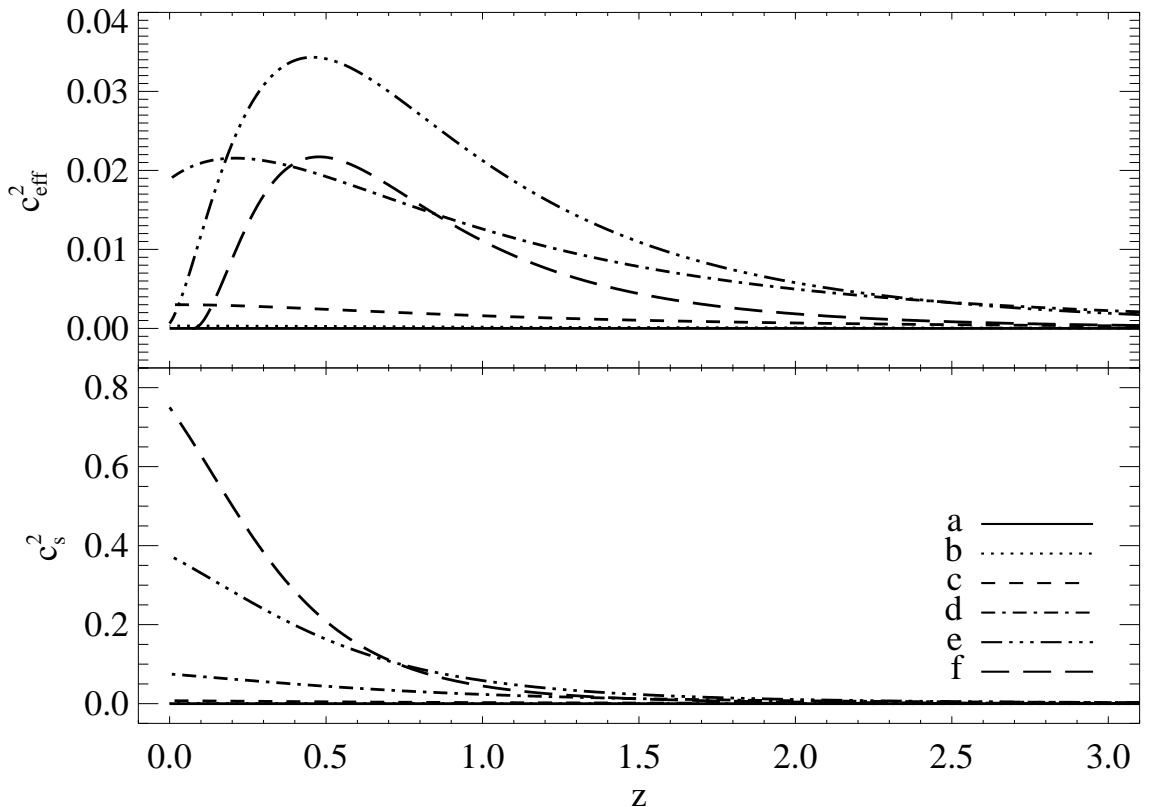


FIG. 3. gCg's c_{eff}^2 and c_s^2 evolution with redshift for all the models presented in Table I. Note that, while the value of c_s^2 increases with the value α , the value of c_{eff}^2 will have much more complex dependence.

system is composed by three equations: two of type (13), one for *baryons* and one for gCg, and one of type (14). The ODE integration was performed by a C++ implementation of a fourth order Runge-Kutta algorithm from $z = 1000$ (at Recombination epoch), to $z = 0$ (the present epoch). The initial conditions (ICs) for the system are $\delta_{g\text{Cg}}(z = 1000) = 3.5 \times 10^{-3}$, $\delta_b(z = 1000) = 10^{-5}$ and $\theta = 0$. The background is described by a flat FLRW universe with density parameters $\Omega_{g\text{Cg}}^0 = 0.95$ and $\Omega_b^0 = 0.05$, and a Hubble constant $H_0 = 72 \text{ kms}^{-1}\text{Mpc}^{-1}$, which are consistent with the latest observational values for the concordance model [38].

We use a TH profile, so pressure gradients are not present, and we can treat *baryons* as dust, i.e. $p_b = w_b = c_{s_b}^2 = c_{\text{eff}_b}^2 = 0$.

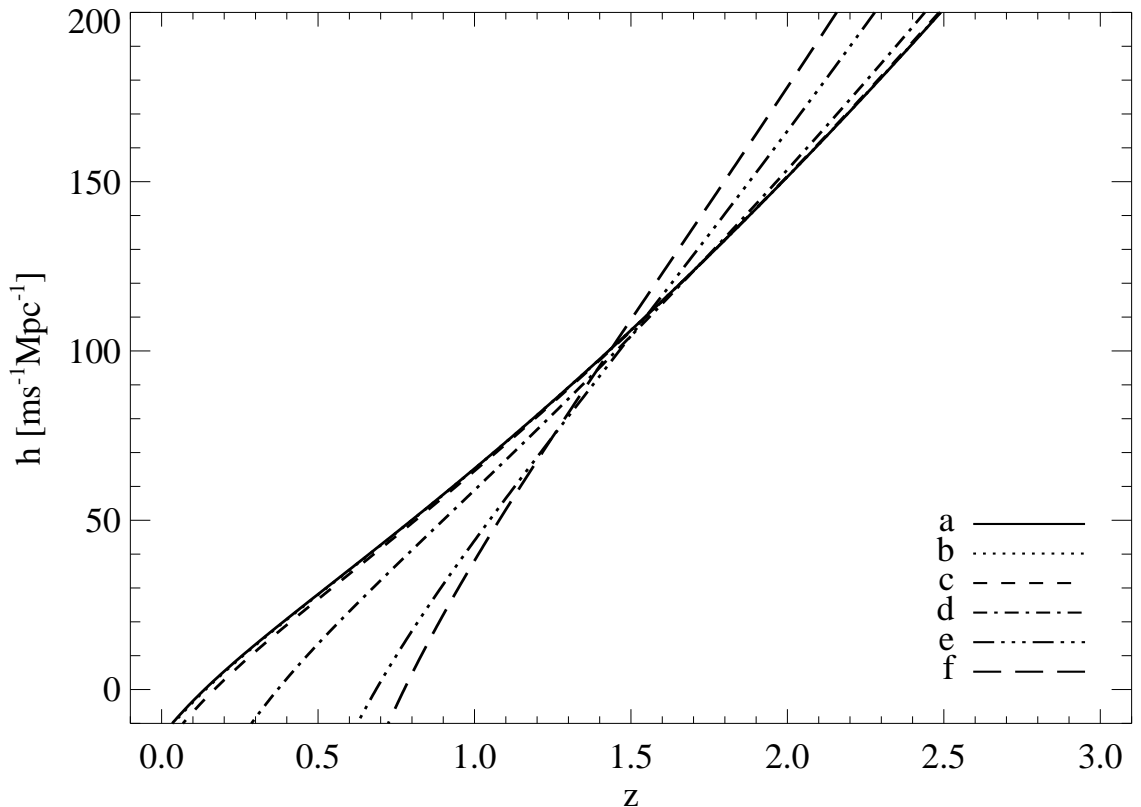


FIG. 4. Collapsed region expansion rate, h , evolution with z . Note that the redshift of turnaround z_{ta} ($h \simeq 0$) is different for each model and for higher values of α it happens at higher redshifts.

B. Results and discussion

When the ICs are the same for all models, the redshift to start the non-linear regime of the collapse, i.e. when $\delta_i \sim 1$, will vary from model to model. The different evolutions for δ , shown in Fig. 1, are the result of the c_{eff}^2 and w own evolutions and their influence on equations (13–14). Not only larger values of α will produce faster collapses, via a larger c_{eff}^2 at lower redshifts, but they also extend the DM stage on the gCg component, thus increasing the collapse in clearly different ways. As is to be expected, this effect is only visible at later times (when DE dominates) and, for most of the time, the perturbation evolution remains undistinguishable between models.

Knowing the δ_{gcg} evolution with scale factor (or z), one can plot the evolution of w_c using Eq. (20) and compare it with the evolution of w . This comparison, illustrated in Fig. 2,

is consistent with the results obtained in Fig. 1, and shows that indeed gCg changes its dynamical nature throughout the collapse. Again, one can see that α has a strong imprint in the results, as higher values of this parameter are connected to a faster collapse, i.e. the value of w_c stays closer to zero throughout the collapse for higher values of α . Eventually, regardless of the choice of α , collapse will occur bringing w_c close to zero. Obviously, this is not always true if one increases \bar{C} too much as that would be the same as increasing the amount of DE in the system, thus preventing collapse altogether.

In Fig. 3 we plot the gCg's c_{eff}^2 and c_s^2 evolution with redshift. Clearly, c_{eff}^2 has a very different evolution when compared to c_s^2 which reinforces the idea that locally the gCg component can behave much differently than that in the background. Contrary to what happens with w_c (see Fig. 2), the value of c_{eff}^2 has a more complex dependence on α . Another imprint, of the influence of α in the dynamics, can be seen in the turnaround epochs (z_{ta}) for the collapsed region (last column of Table I) where higher values of α stand for an earlier turnaround. The turnaround epoch can be defined as the redshift at which h changes sign, from positive to negative values. In Fig. 4, where we show the evolution of h with redshift, it is clear that the higher the value of α is, the faster h decreases and the turnaround point is reached.

It is worth noting that this effect of α in the growth of perturbations is something akin to the SC–TH model. Linear perturbation theory in gCg universes has given results that are partially disagreeing with ours regarding the effect of α in the growth of perturbations (see e.g. [22, 24]). Although this result may seem surprising in fact is something to be expected as we are using a *top-hat* profile for the density (and by extension for the pressure). As the profile is flat no pressure gradient is present in the dynamics and the only mechanism that can suppress growth of perturbations is the accelerated expansion of the universe, which happens only at low redshifts. This limitation can be alleviated if one uses a continuous like profile for the initial perturbation, e.g. gaussian. In this case we can fully quantify the influence of α in the formation of structure, but the use of more complex profiles would imply solving spatial gradients in the dynamic equations.

Finally, we evaluate the influence of ICs in the gCg, ($\delta_{gCg}(z = 1000)$), on the evolution of perturbations, i.e. how the different models in Table I compare if one changes the gCg ICs to obtain the same turn-around redshift for all of them. We considered the turn-around redshift in Model a, $z_{ta} \simeq 0.138$, as the reference one, and force all the others models to

Model	α	\bar{C}	IC ($\times 10^{-3}$)	IC / IC _a
a	0	0.75	3.501	1
b	10^{-3}	0.75	3.498	0.999
c	10^{-2}	0.75	3.468	0.990
d	10^{-1}	0.75	3.219	0.919
e	0.5	0.75	2.635	0.753
f	1	0.75	2.370	0.677

TABLE II. Summary for the turn-around normalization, using the SC-TH framework in gCg-dominated universes.

turn-around at the same epoch.

The implications on the values of the ICs are summarized in Table II. As can be seen, for the turn-around redshift to be the same in all models, no significant changes in the ICs are required. Even in the worst case (Model f), ICs differ only by a factor of ~ 0.677 , which has no meaning, in the context of an unrealistic top-hat scenario as this one.

C. Combined influence of α and \bar{C} on the value of z_{ta}

To understand how z_{ta} depends on both α and \bar{C} , we constructed the plots shown in Fig. 5. As one can see in plot 5(a), z_{ta} is a growing function of α (independently of the value of \bar{C}), with a more pronounced growth for higher values of \bar{C} , as expected. In fact, from Eq. 3, the value of w_{gCg} approaches -1 as \bar{C} tends to 1, which implies that the gCg DE-like behavior dominates over its DM-like behavior, earlier in the system, thus disfavoring the collapse of the perturbation.

On the other hand, high values of α help gCg to keep its pressure closer to zero, extending the collapse stage. As a consequence, when α is large, z_{ta} is almost insensitive to variations of \bar{C} (see plot 5(b)).

IV. CONCLUSIONS

In this paper we studied the growth of perturbations in gCg-dominated universes, using the SC–TH model. The EoS of gCg provides an exact relation for the ratio $\delta p/\delta\rho = c_{eff}^2$ depending on both the redshift and the local density. Based on this relation we showed that, within the SC–TH framework, higher values of α speed up the collapse. This result somehow differs from previous findings obtained in the context of linear theory, e.g. in [21–24]. These results are however not directly comparable to ours, which are derived within the SC–TH framework.

The results obtained here reinforce our expectations on the difference between the global (linear) and local (non-linear) dynamical behavior for the gCg. This can be clearly seen in figures 2 and 3, when comparing the evolution of local parameters w_c and c_{eff}^2 to their background analogous w and c_s^2 .

However, it is worth noting that one should be cautious to take the conclusions obtained here beyond the SC-TH model limitations. In particular neglected effects at the perturbation boundary may invalidate the conclusions [39]. To better quantify the local dynamics of gCg-dominated universes as well the impact of local non-linear inhomogeneities in the background dynamics one would need more realistic profiles as well as adequate numerical methods to handle spatial pressure gradients. We leave those developments to future work.

Appendix: Dynamical Equations

Here we present the derivation of the main equations used in our study. First let us consider the difference between Eq. (6) and Eq. (4),

$$\dot{\rho}_c - \dot{\rho} = 3H(\rho + p) - 3h(\rho_c + p_c), \quad (\text{A.1})$$

which can be expressed in terms of w , w_c , $\delta\rho$ and δ ,

$$\frac{d}{dt}(\delta\rho)/\rho = 3H(1 + w) - 3h(1 + w_c)(1 + \delta), \quad (\text{A.2})$$

and by using Eq. (10) we can also eliminate the variable h ,

$$\frac{d}{dt}(\delta\rho)/\rho = 3H(1 + w) - 3(H + \theta/3a)(1 + w_c)(1 + \delta). \quad (\text{A.3})$$

Adding the relation $\delta\dot{\rho}/\rho = -3H(1 + w)\delta$ to both sides of the equation we get,

$$\frac{d}{dt}(\delta\rho)/\rho - \delta\dot{\rho}/\rho = 3H(1+w) - 3(H + \theta/3a)(1+w_c)(1+\delta) + 3H(1+w)\delta, \quad (\text{A.4})$$

that can be written fully in terms of $\dot{\delta}$ and δ ,

$$\dot{\delta} = 3H(1+w) - 3(H + \theta/3a)(1+w_c)(1+\delta) + 3H(1+w)\delta. \quad (\text{A.5})$$

Recalling that w_c can be expressed in terms of δp , w and δ we can recast last equation as,

$$\dot{\delta} = 3H(1+w) - 3(H + \theta/3a)\left(1 + \frac{w}{1+\delta} + \frac{\delta p}{\rho(1+\delta)}\right)(1+\delta) + 3H(1+w)\delta, \quad (\text{A.6})$$

which then simplifies to,

$$\dot{\delta} = 3H(1+w)(1+\delta) - 3H\left(1 + \delta + w + \frac{\delta p}{\rho}\right) - \left(1 + \delta + w + \frac{\delta p}{\rho}\right)\frac{\theta}{a}. \quad (\text{A.7})$$

Canceling out the last terms we get,

$$\dot{\delta} = 3Hw\delta - 3H\frac{\delta p}{\rho} - \left[1 + \delta + w + \frac{\delta p}{\rho}\right]\frac{\theta}{a}, \quad (\text{A.8})$$

and finally using $\rho = \delta\rho/\delta$ we arrive to the first dynamical equation, (11).

To obtain the second dynamical equation we can start from Eq. (10), to derive the following equality

$$\dot{h} = \dot{H} + \frac{\dot{\theta}}{3a} - \frac{\theta H}{3a} = \frac{\ddot{r}}{r} - h^2 \quad (\text{A.9})$$

which can be written as,

$$\frac{\ddot{r}}{r} = \dot{H} + h^2 + \frac{\dot{\theta}}{3a} - \frac{\theta H}{3a}. \quad (\text{A.10})$$

Inserting Eq. (7) into the previous relation we get,

$$\dot{H} + h^2 + \frac{\dot{\theta}}{3a} - \frac{\theta H}{3a} = -\frac{4\pi G}{3} \sum_i (\rho_{c_i} + 3p_{c_i}) \quad (\text{A.11})$$

where expanding the terms \dot{H} and h^2 we obtain,

$$\frac{\ddot{a}}{a} - H^2 + H^2 + \frac{\theta^2}{3^2 a^2} + \frac{2\theta H}{3a} + \frac{\dot{\theta}}{3a} - \frac{\theta H}{3a} = -\frac{4\pi G}{3} \sum_i (\rho_{c_i} + 3p_{c_i}). \quad (\text{A.12})$$

Finally, removing the extra terms, subtracting the background, and multiplying by $3a$ on both sides we arrive at

$$\dot{\theta} + \theta H + \frac{\theta^2}{3a} = -4\pi G a \sum_i (\delta\rho_i + 3\delta p_i), \quad (\text{A.13})$$

that can be re-written as Eq. (12) by inserting the relations $\delta\rho = \rho\delta$ and $c_{ef}^2 = \delta p/\delta\rho$.

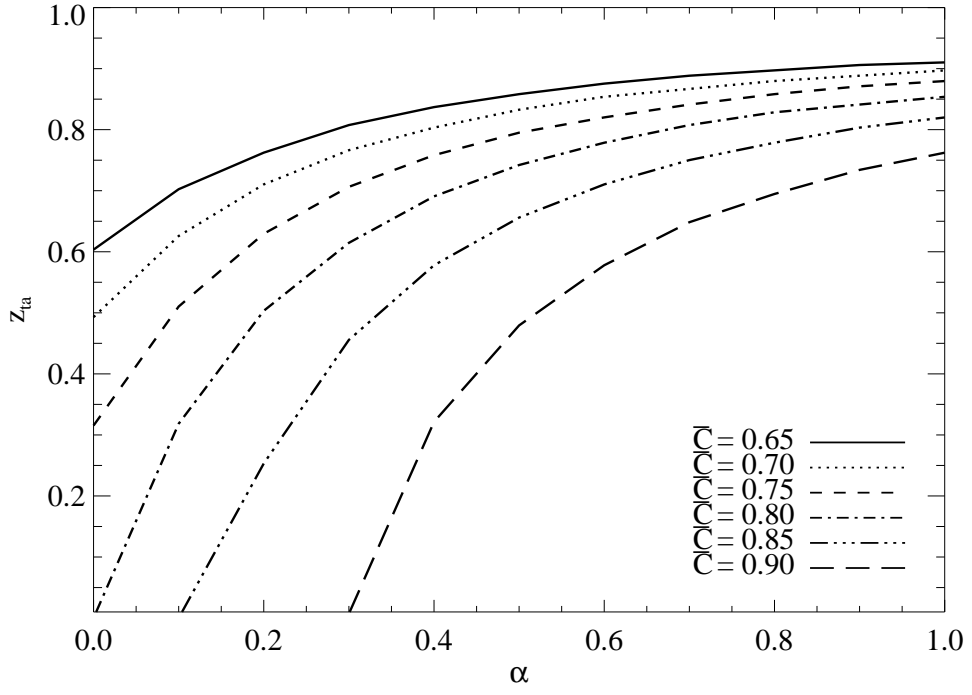
ACKNOWLEDGMENTS

We thank F. Hardt, V. Gorini, P.P. Avelino and O. Bertolami for fruitful discussions. The work of A.K. was partially supported by the RFBR grant No 11-02-00643. AdS is supported by a Ciência 2007 contract, funded by FCT/MCTES (Portugal) and POPH/FSE (EC).

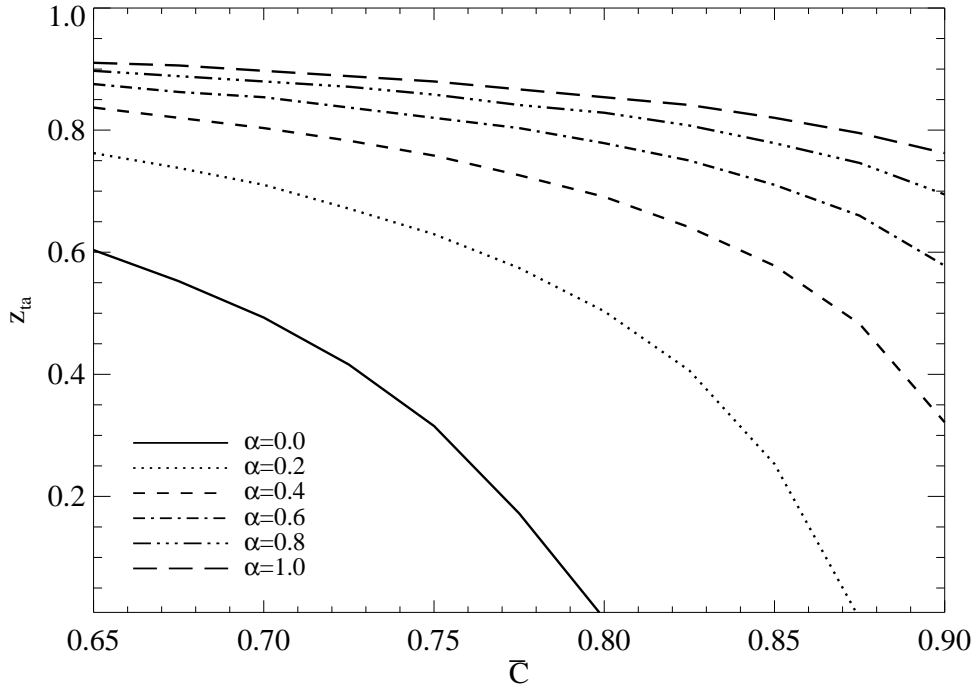
-
- [1] S. Perlmutter *et al.* (Supernova Cosmology Project), *Astrophys. J.* **517**, 565 (1999), [astro-ph/9812133](#).
 - [2] A. G. Riess *et al.* (Supernova Search Team), *Astronomical Journal* **116**, 1009 (1998), [arXiv:astro-ph/9805201](#).
 - [3] J. A. Frieman, M. S. Turner, and D. Huterer, *Annual Review of Astron and Astrophys* **46**, 385 (2008), [arXiv:0803.0982](#).
 - [4] R. R. Caldwell and M. Kamionkowski, *Annual Review of Nuclear and Particle Science* **59**, 397 (2009), [arXiv:0903.0866 \[astro-ph.CO\]](#).
 - [5] J. L. Feng, *Annual Review of Astron and Astrophys* **48**, 495 (2010), [arXiv:1003.0904 \[astro-ph.CO\]](#).
 - [6] K. Garrett and G. Dūda, *Advances in Astronomy* **2011** (2011), [arXiv:1006.2483 \[hep-ph\]](#).
 - [7] B. Gumjudpai, T. Naskar, M. Sami, and S. Tsujikawa, *JCAP* **6**, 7 (2005), [arXiv:hep-th/0502191](#).
 - [8] E. J. Copeland, M. Sami, and S. Tsujikawa, *International Journal of Modern Physics D* **15**, 1753 (2006), [arXiv:hep-th/0603057](#).
 - [9] P. P. Avelino, L. M. G. Beça, and C. J. A. P. Martins, *Phys. Rev. D* **77**, 063515 (2008), [arXiv:0711.4288](#).
 - [10] D. Bertacca, N. Bartolo, and S. Matarrese, *Advances in Astronomy* **2010** (2010), 10.1155/2010/904379, [arXiv:1008.0614 \[astro-ph.CO\]](#).
 - [11] A. Kamenshchik, U. Moschella, and V. Pasquier, *Phys. Rev. B* **511**, 265 (2001), [arXiv:gr-qc/0103004](#).
 - [12] N. Bilić, G. B. Tupper, and R. D. Viollier, *Physics Letters B* **535**, 17 (2002), [arXiv:astro-ph/0111325](#).

- [13] M. C. Bento, O. Bertolami, and A. A. Sen, *Phys. Rev. D* **66**, 043507 (2002), [arXiv:gr-qc/0202064](#).
- [14] V. Gorini, A. Kamenshchik, and U. Moschella, *Phys. Rev. D* **67**, 063509 (2003), [arXiv:astro-ph/0209395](#).
- [15] S. Chaplygin, *Sci. Mem. Moscow Univ. Math. Phys* **21**, 1 (1901).
- [16] P. P. Avelino, L. M. Beça, J. P. de Carvalho, C. J. Martins, and P. Pinto, *Phys. Rev. D* **67**, 023511 (2003), [arXiv:astro-ph/0208528](#).
- [17] R. Bean and O. Doré, *Phys. Rev. D* **68**, 023515 (2003), [arXiv:astro-ph/0301308](#).
- [18] R. Colistete, J. C. Fabris, S. V. B. Gonçalves, and P. E. de Souza, *International Journal of Modern Physics D* **13**, 669 (2004), [arXiv:astro-ph/0303338](#).
- [19] T. Barreiro, O. Bertolami, and P. Torres, *Phys. Rev. D* **78**, 043530 (2008), [arXiv:0805.0731](#).
- [20] N. Liang, L. Xu, and Z. Zhu, *A&A* **527**, A11+ (2011), [arXiv:1009.6059 \[astro-ph.CO\]](#).
- [21] L. M. Beça, P. P. Avelino, J. P. de Carvalho, and C. J. Martins, *Phys. Rev. D* **67**, 101301 (2003), [arXiv:astro-ph/0303564](#).
- [22] H. B. Sandvik, M. Tegmark, M. Zaldarriaga, and I. Waga, *Phys. Rev. D* **69**, 123524 (2004), [arXiv:astro-ph/0212114](#).
- [23] P. P. Avelino, L. M. Beça, J. P. de Carvalho, C. J. Martins, and E. J. Copeland, *Phys. Rev. D* **69**, 041301 (2004), [arXiv:astro-ph/0306493](#).
- [24] V. Gorini, A. Y. Kamenshchik, U. Moschella, O. F. Piattella, and A. A. Starobinsky, *JCAP* **2**, 16 (2008), [arXiv:0711.4242](#).
- [25] N. Bilic, R. J. Lindebaum, G. B. Tupper, and R. D. Viollier, *JCAP* **11**, 8 (2004), [arXiv:astro-ph/0307214](#).
- [26] A. V. Macciò, C. Quercellini, R. Mainini, L. Amendola, and S. A. Bonometto, *Phys. Rev. D* **69**, 123516 (2004), [arXiv:astro-ph/0309671](#).
- [27] N. Aghanim, A. C. da Silva, and N. J. Nunes, *A&A* **496**, 637 (2009), [arXiv:0808.0385](#).
- [28] M. Baldi, V. Pettorino, G. Robbers, and V. Springel, *MNRAS* **403**, 1684 (2010), [arXiv:0812.3901](#).
- [29] B. Li, D. F. Mota, and J. D. Barrow, *Astrophys. J.* **728**, 109 (2011), [arXiv:1009.1400 \[astro-ph.CO\]](#).
- [30] T. Multamäki, M. Manera, and E. Gaztañaga, *Phys. Rev. D* **69**, 023004 (2004), [arXiv:astro-ph/0307533](#).

- [31] F. Pace, J. Waizmann, and M. Bartelmann, *MNRAS* **406**, 1865 (2010), [arXiv:1005.0233 \[astro-ph.CO\]](#).
- [32] L. R. Abramo, R. C. Batista, L. Liberato, and R. Rosenfeld, *Phys. Rev. D* **77**, 067301 (2008), [arXiv:0710.2368](#).
- [33] J. E. Gunn and J. R. Gott, III, *Astrophys. J.* **176**, 1 (1972).
- [34] T. Padmanabhan, *Structure Formation in the Universe*, edited by Padmanabhan, T. (1993).
- [35] D. F. Mota and C. van de Bruck, *A&A* **421**, 71 (2004), [arXiv:astro-ph/0401504](#).
- [36] L. R. Abramo, R. C. Batista, L. Liberato, and R. Rosenfeld, *Phys. Rev. D* **79**, 023516 (2009), [arXiv:0806.3461](#).
- [37] W. Hu, *Astrophys. J.* **506**, 485 (1998), [arXiv:astro-ph/9801234](#).
- [38] E. Komatsu, K. M. Smith, J. Dunkley, C. L. Bennett, B. Gold, G. Hinshaw, N. Jarosik, D. Larson, M. R.olta, L. Page, D. N. Spergel, M. Halpern, R. S. Hill, A. Kogut, M. Limon, S. S. Meyer, N. Odegard, G. S. Tucker, J. L. Weiland, E. Wollack, and E. L. Wright, *Astrophysical Journal Supplement* **192**, 18 (2011), [arXiv:1001.4538 \[astro-ph.CO\]](#).
- [39] N. Bilić, G. B. Tupper, and R. D. Viollier, *Phys. Rev. D* **80**, 023515 (2009), [arXiv:0809.0375 \[gr-qc\]](#).



(a)



(b)

FIG. 5. Dependence of z_{ta} on the parameters α and \bar{C} . *Top:* z_{ta} vs α for different values of \bar{C} . *Bottom:* z_{ta} vs \bar{C} for different values of α .